# Residual capacity assessment of reinforced concrete D-Regions affected by corrosion

Hernández-Montes, E.[a]; Fernández-Ruiz, M.A.[b]; Carbonell-Márquez, J.F.[c]; Gil-Martín, L.M.[d]

[a] Department of Structural Mechanics, University of Granada (UGR). Campus Universitario de Fuentenueva s/n. 18072 Granada, Spain. emontes@ugr.es

[b] Department of Industrial and Civil Engineering, University of Cádiz (UCA). Campus Bahía de Algeciras, Avda. Ramón Puyol, s/n. 11201 Algeciras (Cádiz), Spain. manuelalejandro.fernandez@uca.es

[c] Departamento de Mecánica, Universidad de Córdoba. Campus de Rabanales, Edificio Leonardo da Vinci, E-14071 Córdoba, Spain. jcarbonell@uco.es

[d] Department of Structural Mechanics, University of Granada (UGR). Campus Universitario de Fuentenueva s/n. 18072 Granada, Spain. mlgil@ugr.es

## Abstract

The repair and rehabilitation of Reinforced Concrete (RC) structures affected by the corrosion of their reinforcement is a complex task. The estimation of the residual structural capacity of corroded RC structures is becoming a crucial factor in the decision-making process of repair or demolition. Many researchers have studied the effects of reinforcement corrosion on the load capacity of RC beams (Bernoulli or B-Regions) but little attention has been paid to disturbed or D-Regions. This piece of work presents a procedure for the assessment of the residual structural capacity of D-Regions in RC members. The bond deterioration between steel and concrete, the reduction of the cross-sectional area of reinforcement, the deterioration of the concrete area of the cross-section and the softening of concrete has been taken into consideration. The accuracy of the method has been tested with experimental results which exist in relevant literature.

**Keywords:** Disturbed regions. Reinforced concrete. Corroded reinforcement. Residual capacity. Anchorage length.

## 1. Introduction

Despite having many advantages, Reinforced Concrete (RC) members have one very significant weakness: corrosion of steel reinforcement. More than a few RC structures have been demolished before the end of their originally estimated useful life due to the corrosion of reinforcement and numerous corroded RC structures are currently in service, with or without being repaired. In this regard, the inspection, repair and rehabilitation of existing RC structures affected by corrosion have become very important in construction. Accordingly, the assessment of the residual capacity of a corroded RC structure is a key task that reflects the current state of the structure.

Under normal circumstances, concrete provides protection to reinforcing steel through both its high alkalinity (chemical protection) and its dense and relatively impermeable structure (physical protection). The corrosion rate of rebars shows the efficiency of protection against corrosion [1]. Corrosion is caused by the attack of chloride ions that penetrate into the concrete matrix or by the carbonation of the concrete cover (or a combination of both). The carbonation and/or chloride attacks cause the alkaline concrete environment to deteriorate, disrupting the thin oxide layer that covers the steel bars (known as the passive layer). This is the starting point of the corrosion process. Among many other negative effects, corrosion causes a reduction of the cross-sectional area of reinforcing bars [2], cracking of the concrete cover [3], reduction of the bond strength between the reinforcing steel and the concrete [4–6] and softening of the concrete [7]. All these effects acting together can weaken RC structures, thereby reducing their load-carrying capacity and their service lives. Authors present a holistic analysis of the deterioration due to the corrosion of D-Regions as a function of the crack width in such a way that it provides the residual capacity of the D-Region. This has not been performed before and is presented in this work.

The structural evaluation of an existing RC structure is a complex task. The use of Destructive and Non-Destructive Tests (DT and NDT, respectively) in the determination of the current conditions of RC members increases the accuracy of structural evaluation. However, in most cases, the use of DT is not possible due to the length of time it takes and the damage caused to a structure. To a lesser extent, something similar occurs with NDT[8]. In this case it is because most of these tests require special equipment and techniques that are often not readily available[9,10]. Numerical analyses have also been applied to study the crack propagation, particularly in layered materials as in[11,12]. On the other hand, deterioration indicators such as concrete cracks and the loss of concrete cover can easily be evaluated by visual inspection or using simple NDT. This information provides the engineer with crucial information about the real state of the structure.

An important aspect to be considered when applying an assessment method of the load capacity of a potentially corroded structure is the type of region to be studied. It is known that all RC structures consist of D (Disturbed or Discontinuity) and B (Bernoulli or Beam) regions. In B-Regions it is assumed that plane sections remain plane after deformation (linear strain distribution) whereas the strain distribution in D-Regions is significantly nonlinear [13].

The design of B-Regions is well established in current structural practice codes, such as the European [14] and North American ones [15], based on the classic beam theory. D-Regions, which occur in zones close to corners, supports and concentrated loads such as corbels and deep beams, can be designed with Finite Element Analysis (FEA) as in [16] or alternatively with the Strut and Tie Method (STM)[13,17]. The STM is a design method based on the lower-bound theorem of limit analysis for D-Regions in RC structures. This method idealizes the structural behavior of a particular D-Region as a system of struts (compression members) and ties (tension members) connected in nodes (nodal zones). STM is included in Eurocode 2 (EC2) [14], AASTHO Bridge Design Specifications [18] or ACI-318 [15]where some conditions on the definition of the truss and on the calculation of the capacity and dimensions of its members are established. Even though reinforcement corrosion has a considerable impact on the structural behavior of both B- and D-Regions, the effect of corrosion on the residual capacity of B-Regions has been covered much more extensively in relevant literature[7,19–21] than that of D-Regions[22,23].

In Carbonell-Márquez et al. [20] authors proposed a procedure for the assessment of the residual capacity of corroded B-Regions. In the present work, which corresponds to the second part of the research, a procedure for the assessment of the residual capacity of D-Regions in existing RC structures with corroded reinforcement is proposed. The inputs of the method are the non-deteriorated or initial state of the structure (geometry and reinforcement layout) and the actual geometry, properties of materials and corrosion crack map (distribution and widths of the main concrete cracks due to corrosion). The method is presented in detail together with an example. Finally, the proposed procedure is verified by the comparison of its results with the corresponding ones from experimental results existing in relevant literature. The present study, in conjunction with the previous analysis of B-Regions, allows the effect of the corrosion in the actual capacity of concrete structures to be evaluated.

## 2. Structural modelling of corrosion effects in D-Regions

All the corrosion-induced negative effects considered in the analysis of a corroded D-Region are explained separately. All the aspects involved in the deterioration of D-Regions can be expressed in terms of the geometry and the cracking pattern (i.e.

distribution and widths of the main corrosion cracks) of the RC member as described in the following subsections.

## 2.1. Loss of cross-sectional area of steel rebars

A direct consequence of steel corrosion is the loss of the cross-sectional area of rebars. The corrosion of the reinforcement can occur in an uniform form and/or in a localized form [24]. Uniform corrosion (the most common type) leads to a homogeneous steel cross-section reduction. On the other hand, localized corrosion or pitting consists of a local iron dissolution that produces holes and cavities in the bar. This last type of corrosion may cause a higher radial pressure on the surrounding concrete than with the uniform one, accelerating the corrosion process [24]and making it more difficult to detect and prevent.

The corrosion level, $\chi$, is usually calculated by using the original or uncorroded mass $m$ of the rebar and the corresponding mass after the corrosion process $m_{corr}$ obtained by removing the corrosion products, see Eq. (1).

$$\chi = \frac{m - m_{corr}}{m} \tag{1}$$

Therefore, assuming as constant the steel density, the reduction of cross-sectional area, $\Delta A_s$, of the corroded steel bar is determined as a function of its corrosion level $\chi$ as:

$$\Delta A_s = A_s - A_{corr} = \chi A_s \Rightarrow A_{corr} = A_s(1-\chi) \tag{2}$$

where $A_s$ and $A_{corr}$ are the uncorroded and corrosion-affected rebar areas, respectively. According to this, the corrosion-affected rebar diameter $\phi_{corr}$ can be expressed as:

$$A_{corr} = A_s - \Delta A_s = A_s(1-\chi) \Rightarrow \phi_{corr} = \phi\sqrt{1-\chi} \tag{3}$$

with $\phi$ the diameter of the uncorroded steel bar.

In existing RC structures, the use of Eq. (3) to estimate the corrosion level would imply the careful extraction of bars or coupons from the corroded member, which is risky, costly and time consuming. Hence, an indirect computation of the corrosion level $\chi$ based on data obtained by a simple visual inspection of the corroded structure is very interesting from a practical point of view. Experimental results in the literature show that the surface crack width is closely related with the corrosion level of the steel bars[25,26]. Based on the results of two naturally corroded RC beams in a saline environment, subjected to wetting and drying cycles over periods of 14 and 17 years, Vidal et al. [26] proposed an empirical expression that relates the corrosion-induced rebar cross-section reduction $\Delta A_s$ ($mm^2$) to the width of corrosion-induced longitudinal cracks, $w$ (mm):

$$w = 0.0575\left(\Delta A_s - \Delta A_0\right) \tag{4}$$

where $\Delta A_{s0}$ is the reduction of the area of the cross section that initiates cracking expressed in $mm^2$. As defined $\Delta A_s$, in Eq. (2), $\Delta A_{s0}$ can be also expressed as a function of the corrosion level that initiates corrosion cracking $\chi_0$ (i.e. $\Delta A_{s0} = \chi_0 A_s$).

Finally, Eq. (4) can be combined with Eq. (2) in order to obtain a relationship between the corrosion level, $\chi$, and the width of corrosion-induced longitudinal cracks, $w$(mm):

$$w = 0.0575 A_s\left(\chi - \chi_0\right) \leftrightarrow \chi = \frac{w}{0.0575 A_s} + \chi_0 \tag{5}$$

Rodríguez et al. [2] proposed a model that correlates the loss of cross-sectional area with the corrosion attack penetration or reduction of the radius of the cross-sectional rebar $y$ so that the effective diameter of a rebar can be expressed as:

$$\phi_{corr} = \phi - \alpha y \tag{6}$$

where $\alpha$ is a corrosion parameter with value equal to 2 in case of uniform corrosion and with value between 4 and 8 in case of pitting corrosion [27] (see Figure 1). Naming $y_0$ as the value of the attack penetration that initiates cracking, combining Eqs. (3) and (6), a relationship between $y_0$ and the corresponding corrosion level $\chi_0$ can be stated:

$$\chi_0 = 1 - \left(1 - \frac{\alpha\, y_0}{\phi}\right)^2 \tag{7}$$

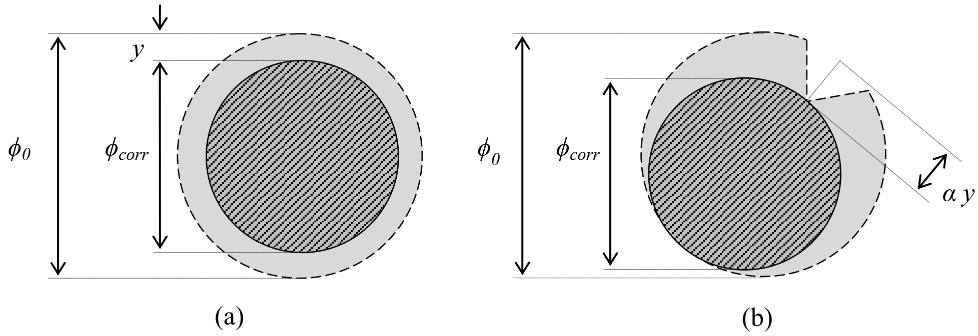


**Figure 1. Reduced section of the steel bar produced by uniform (a) and localized (b) corrosion. Adapted from [2].**

Alonso et al. [28] proposed an empirical formulae to obtain the corrosion penetration that initiates cracking, $y_0$ (mm), as a function of the distance between the outer surface of the concrete and the corroded longitudinal steel bar $c$ (mm) and the uncorroded diameter $\phi$ (mm):

$$y_0 = \left(7.53 + 9.32\frac{c}{\phi}\right)10^{-3} \tag{8}$$

Finally, combining now Eqs. (5), (7) and (8) the corrosion level can be estimated based on information about the original reinforcement configuration ($c$ and $\phi$) and visual inspection($w$) as:

$$\chi = \frac{w}{0.0575A_s} + 1 - \left[1 - \frac{\alpha}{\phi}\left(7.53 + 9.32\frac{c}{\phi}\right)10^{-3}\right]^2 \tag{9}$$

with $w$, $c$ and $\phi$ expressed in mm and $A_s$ in mm$^2$. Once the corrosion level $\chi$ is estimated, the loss of cross-section of the corroded rebar $A_{corr}$ can be calculated by means of Eq. (2).

## 2.2.Bond strength model for corroded bars

Eurocode 2 provides formulation to design or evaluate the anchorage in sound reinforced concrete members. According to this standard, the design anchorage length$l_{bd}$

(all the correction factors equal to 1) for a rebar with diameter $\phi$ is:

$$l_{bd} = \frac{\phi \sigma_{sd}}{4 f_{bd}} \tag{10}$$

where $\sigma_{sd}$ is the design stress of the reinforcing bar at the anchorage section and $f_{bd}$ is the ultimate bond stress, defined in EC2 as:

$$f_{bd} = 2.25 \eta_1 \eta_2 f_{ctd} \tag{11}$$

In Eq. (11), $f_{ctd}$ is the design value of the concrete tensile strength, $\eta_1$ is a coefficient related to the quality of the bond condition and the position of the bar during concreting and $\eta_2$ is a coefficient related to the diameter of the rebar.

A direct result of corrosion is the modification of the anchorage capacity of rebar given the reduction of bond strength. Many different models to relate bond strength with corrosion of reinforcement have been proposed by researchers[25,29,30]. Barghava et al. [31,32] proposed an empirical model based on data from flexural tests of specimens with stirrups (Al-Sulaimani et al.[33]) and without stirrups (Stanish et al. [6]and Chung et al. [4]), see Figure 2 and Eq.(12).

$$f_{bd,corr}(\chi) = R\, f_{bd} = \begin{cases} f_{bd} & \text{for } \chi \le 1.5\% \\ 1.346\ e^{-0.198\chi} f_{bd} & \text{for } \chi > 1.5\% \end{cases} \tag{12}$$

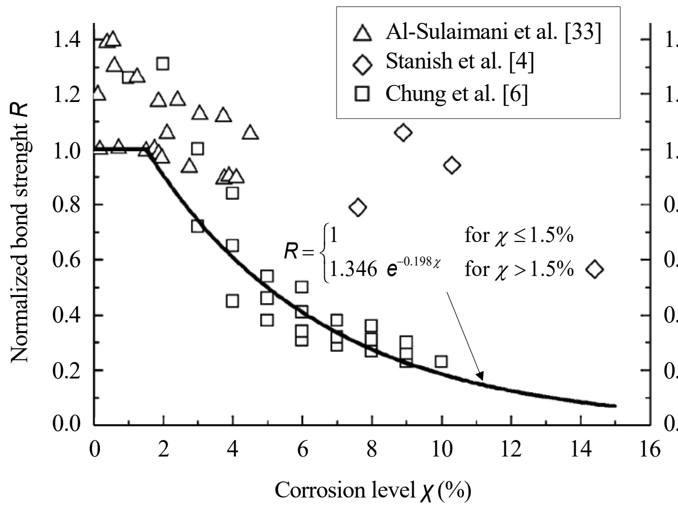


**Figure 2. Normalized bond strength $R$ as a function of corrosion level $\chi$ for experimental data of flexural tests. Adapted from [31,32].**

The normalized bond strength $R$ in Eq. (12) is defined as the ratio of the corrosion affected bond strength ($f_{bd,corr}$) to the original bond strength ($f_{bd}$), see Eq. (13).

$$f_{bd,corr} = R\, f_{bd} \tag{13}$$

Model Code 2010 (MC2010) [34] proposed a reduction of the bond strength of corroded reinforcement in function of the corrosion-induced crack width $w$. In Figure 3, the normalized bond strength $R$ (in percentage) obtained from Eq.(12) and the upper and lower limits proposed by MC2010 have been plotted against the corrosion crack width for comparison. In Figure 3, Eq.(12) has been plotted in conjunction with Eq. (9) for c=30mm, α=2 and ϕ=20, 25 and 32 mm.

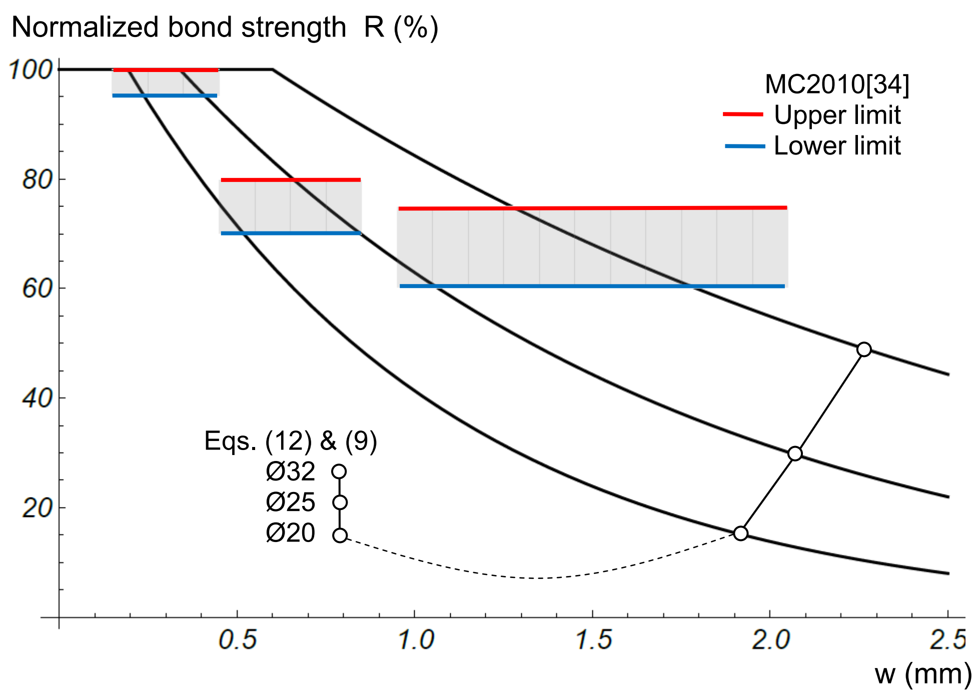


**Figure 3. Comparison of the model proposed by Barghava et al. [31,32] and MC2010 [34].**

It can be seen in Figure 3 that the normalized bond strength given by Eq.(12) is almost the same than the one proposed by MC2010 for $w \leq 0.4$ mm. For high degree of corrosion, the limits established by MC2010 are considerably greater than the value obtained from Eq.(12) whereas than for values of crack widths in the range 0.4 - 0.6 mm Eq.(12) overestimates the residual bond stress respect of the MC2010. Without loss of generality, the expression for the normalized bond strength given by Eq.(12) has been adopted here.

In the expression of the anchorage length given by Eq.(10), two parameters are susceptible to be affected by corrosion: the diameter of the rebar and the bond strength, which are reduced according to Eq.(3) and Eq.(13), respectively. The corrosion-affected anchorage length, $l_{bd,corr}$, can be obtained from Eq. (10) as:

$$l_{bd,corr} = \frac{\phi_{corr}}{4} \frac{\sigma_{sd,corr}}{f_{bd,corr}} \tag{14}$$

where $\sigma_{sd,corr} \leq f_{yd}$ is the design stress of the reinforcing bar at the anchorage section but affected by corrosion. From a structural point of view, the effect of corrosion can be balanced by increasing the anchorage length [20] but this is not always possible. Such is the case of D-Regions, in which the anchorage length $l_b$ is limited by the available distance as it is shown in Figure 4. For this reason, the way which has been proposed for estimating the loss of bond strength due to corrosion in D-Regions is by calculating the maximum stress that the reinforcing bar can withstand with the actual anchorage length, $l_b$ (see Figure 4), but in corroded conditions, $\sigma_{sd,corr}$ (see Eq. (15)).

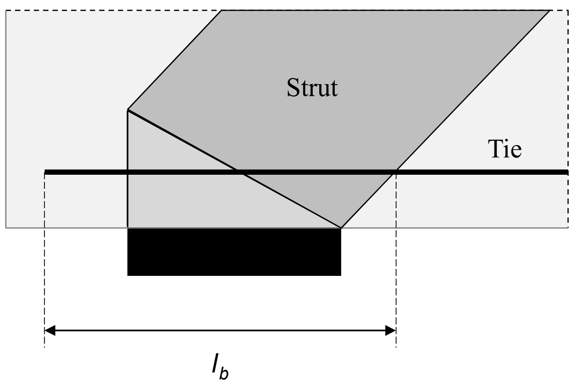


**Figure 4. Example of available anchorage length limited by the geometry of STM.**

$$\sigma_{s,corr} = Min\left( \frac{4}{\phi_{corr}} l_b f_{bd,corr} ; f_{yd} \right) \tag{15}$$

In Eq. (15) an upper limit has been imposed because the value of $\sigma_{sd,corr}$ cannot be higher than the yield stress of the reinforcement bar, $f_{yd}$.

It should be considered that the bond strength loss considered in this section indirectly supposed uniform corrosion. A safe assumption for the case of localized corrosion.

### 2.3. Softening effect in cracked concrete

Uncracked compressed concrete has exhibited higher compressive strength and stiffness than cracked concrete in compression [35]. This effect, called compression softening, is related to the principal tensile strain$\varepsilon_1$ and average tensile strain $\varepsilon_3$ (see Figure 5 (a) and (b)). Both tensile strains form a right angle with the direction of the principal compression strain $\varepsilon_2$ causing cracking. In the particular case of D-Regions, Tjhin and Kuchma [36] stated that any disturbance in the struts significantly affects their capacity. These disturbances include initial cracks, parallel or inclined, in the strut axis and tensile transverse stress or strain (such as that produced by a crossing tie).

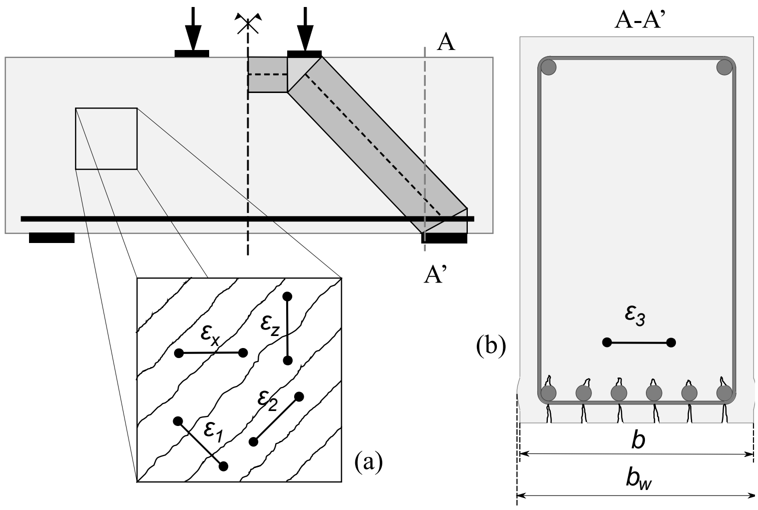


**Figure 5. Average strains in a cracked RC element. Example of D-Region (deep beam): (a) strain perpendicular $\varepsilon_1$ and parallel $\varepsilon_2$ to the concrete strut axis; (b) average concrete strain at plane of cross-section $\varepsilon_3$.**

Corrosion-induced softening is mainly associated with the average tensile strain $\varepsilon_3$ (perpendicular to the principal compressive strain $\varepsilon_2$, see Figure 5 (b)) produced by rust accumulation which causes longitudinal micro-cracks [7]. According to Coronelli and Gambarova [7], the compressive strength of concrete affected by softening due to corrosion cracking $f_c^*$ is given by the following expression:

$$f_c^* = \zeta_{corr} f_c \tag{16}$$

where $\zeta_{corr}$ is a factor called softening coefficient defined as:

$$\zeta_{corr} = \frac{1}{1 + K\dfrac{\varepsilon_3}{\varepsilon_{c0}}} \tag{17}$$

In Eq. (17), $K$ is a coefficient related to the roughness of the bar and its diameter (according to Capè [37] $K$ = 0.1 for medium-diameter ribbed bars) and $\varepsilon_{c0}$ is the concrete strain corresponding to the peak compressive stress $f_c$.

According to Coronelli and Gambarova [7], the strain $\varepsilon_3$ can be calculated as:

$$\varepsilon_3 = \frac{b_w - b}{b} \approx \frac{\sum w_i}{b} \tag{18}$$

where $b_w$ is the increased width by corrosion cracking (see example of a deep beam cross-section shown in Figure 5 (b)). The increase of the width of a D-Region ($b_w - b$) can be approximated by the sum of all the longitudinal crack widths $w_i$ formed during the corrosion of the longitudinal reinforcing bars which intersect the strut.

### 2.4. Reduction of the concrete area

Rust products formed during the corrosion of reinforcement can cause internal stresses on concrete due to its volume expansion. This internal pressure results in concrete cover cracking, delamination and spalling [38–40] that reduce the concrete area. Consequently, the effective dimensions of the RC element must be considered in order to account for these effects.

Empirical formulations can be used to calculate the non-damaged cross-sectional area of concrete. One of these empirical expressions is the one proposed by Higgins et al. [41]

from which the effective width, $b_{eff}$ (see Figure 6), is obtained as function of the original undamaged beam width ($b$), the concrete cover ($c$), the stirrup diameter ($\phi_{st}$) and the stirrup spacing ($s_{st}$):

$$\begin{aligned} b_{eff} &= b - 2\left(c + \phi_{st}\right) + \frac{s_{st}}{5.5} \quad && if \ s_{st} \leq 5.5c \\ b_{eff} &= b\frac{5.5}{s_{st}}\left(c + \phi_{st}\right)^{2} \quad && if \ s_{st} > 5.5c \end{aligned} \tag{19}$$

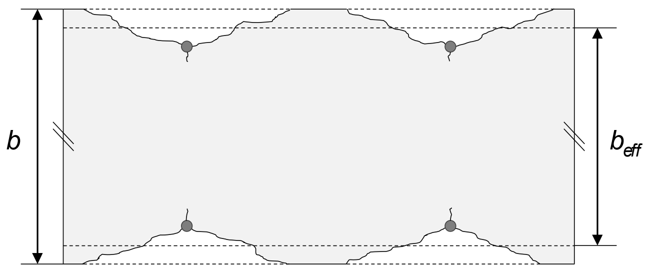


**Figure 6. Plan view of concrete cracking due to corrosion.**

In Eq. (19) all the dimensions are in inches (1 in= 25.4 mm). Certain precautions should be taken when using empirical formulations in order to guarantee their suitability for each particular case.

## 3. Critical review of the struts design in the STM methodology

In the proposed method it is considered that the reinforcement layout is known when evaluating the capacity of a particular D-Region. Consequently, the location of the ties is initially defined. In order to determine the geometry of the struts and the nodes two different criteria can be followed. In the first criterion the width of the struts is defined supposing that they are working at the concrete strength capacity (§7.3.6.2 of the Model Code 2010[34]). On the other hand, the second criterion does not explicitly account for the struts dimensions based on that the struts are stronger than the nodes: "Since the compressive stress will be highest at a node there is no need to investigate compression elsewhere in the strut", from §C.5.8.2.2 AASHTO LRFD-8 [18].

Following AASHTO methodology, nodes are designed according to purely geometrical conditions: bearing dimensions, reinforcement location and depth of the compression zone calculated in the interface with the B-Region. The AASHTO philosophy is backed by the classical Kani's campaign [42] and the experience of the authors [43]. Nevertheless, the latest version of the AASHTO LRFD-8 Bridge Design (2017), with respect to the previous version of 2012, has modified some of the nodal geometries and has removed the criteria for the effective breadth of the struts.

A close look to the formulation proposed by MC2010[34] and Eurocode 2[14] reveals that, except for one case, the reduced concrete compressive strength in struts is always smaller than in nodes. In this sense no formulation should be needed but just the AASHTO LRFD-8 assertion quoted above. The said exception is for the case where the struts is located in an undisturbed uniaxial compression stress state or in a region with transverse compression.

In view of the aforementioned two options can be taken for the assessment and design of the struts dimensions: 1) suppose the dimensions suggested by AASHTO and check that demanded stresses are smaller than the capacity or 2) suppose the dimensions deduced from the capacity. The former has been taken in this work.

## 4. Capacity of the D-Region.

An example from Hernández-Montes and Gil-Martín [44] has been taken to better explain the procedure proposed for the assessment of the residual capacity of D-Regions in RC structures. Figure 7 shows the reinforcement layout and the dimensions of the nodes and the struts. These dimensions have been deduced according AASHTO LRFD-8 [18]. A detailed explanation for a similar case can be seen in Martin and Sanders [45], although they followed a former version of the same specifications.

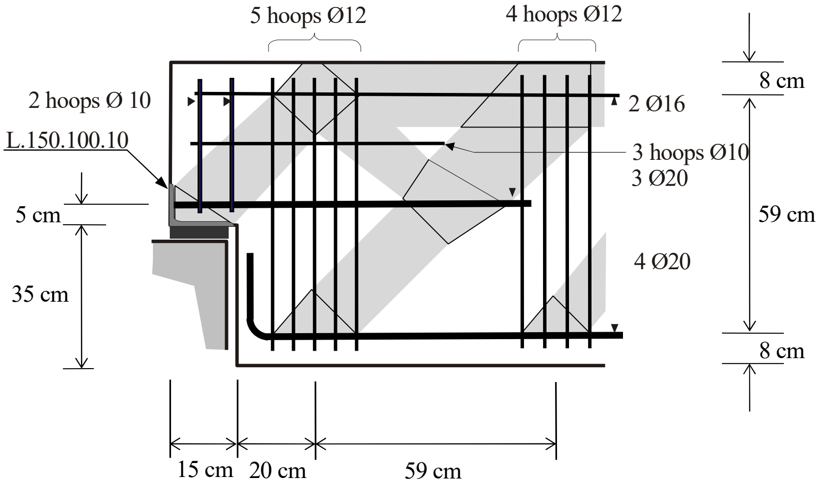


**Figure 7. Reinforcement layout.**

Figure 8 shows the Strut and Tie (S&T) model of the D-Region. The thickness of strut CD is designed following the AASHTO description of CTT nodes, applied to node C. Strut BE has been supposed to be centered at 8 cm from the top, so that the thickness of strut BE is 16 cm. For a fixed value of *P* (see Figure 8) the thickness of strut BE can be calculated, being the depth of the compression zone. As *P* is considered to be a variable, strut BE thickness could be also a variable, nevertheless in the present work and without loss of generality it has been considered as a constant. Thickness of strut BE and geometry of tie EF define the thickness of strut DE. Geometry of the tie AD and thicknesses of struts CD, DE and BE define thickness of strut BD. Geometry of support A and thicknesses of struts BD define strut AB (see Figure 8).

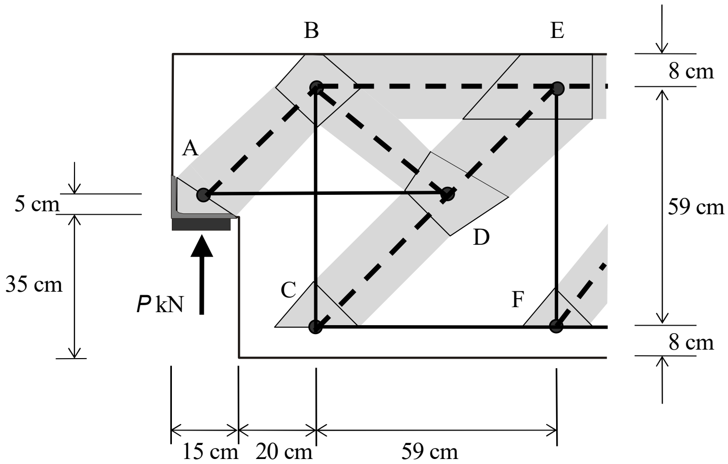


**Figure 8. S&T model of the example depicted in Figure 7.**

Solving the S&T model, the axial force $N$ acting on each one of the strut or tie can be expressed as a function of $P$, i.e. $N_i=\delta_i P$, being $i$ the number of the strut or tie, see Table 1, where negative sign means tension and positive sign compression.

**Table 1. Forces in the truss structure**

| | AB | AD | BC | BD | BE | CD | CF | DE | EF |
|---|---|---|---|---|---|---|---|---|---|
| Axial Force $N_i=\delta_i P$ (kN) | 1.43 P | -1.02 P | -1.47 P | 0.72P | 0.47 P | 2.07P | -1.47 P | 1.41P | -1.00 P |

### 4.1. Capacity evolution of the ties

The decay of the capacity of the ties is due to effects described in Subsections 2.1 (loss of area of the rebar as function of the crack width $w$) and 2.2 (reduction of the bond stress, function of $w$)of the present work.

Evolution of the capacity of the ties due to the loss of cross section as function of the crack width ($w$) is calculated following the expression:

$$\left.\begin{array}{l} P_i(w) = N_i(w)/\delta_i \\ N_i(w) = f_{yd} A_{i,corr}(w) \\ A_{i,corr}(w) = (1-\chi(w))A_s \end{array}\right\} \rightarrow P_i(w) \tag{20}$$

The expression of the corrosion level $\chi(w, A_s, \phi)$ is given by Eq. (9). For each one of the ties the $A_s$ and $\phi$ are the initial values of both area and diameter of the reinforcement, respectively. Because $A_s$ and $\phi$ are constant $\chi$ is only function of crack width $w$, i.e. $\chi(w)$.

Evolution of the capacity of the ties due to decay of the bond because of corrosion is calculated supposing that anchorage length do not vary but the bond stress decreases taking the value of $f_{bd,corr}$. Anchorage of vertical ties (EF and BC) fulfils prescriptions for anchorage of links and shear reinforcement (e.g. EC2 §8.5) so that deterioration of bond is only considered for the AD and CF ties.

The evolution of the capacity due to both loss of cross-section and to bond deterioration of ties can be observed in Figure 9. The flatter part of the curves corresponding to AD and CF ties shows the behavior due to the loss of cross-sectional area. The steepest part of these curves corresponds to bond deterioration. Ties EF and BC show steeper curves than the flatter parts of curves AD and CF because these reinforcing bars are of smaller diameter, and the loss of cross-sectional area is greater for the same crack width.

It is assumed that concrete cover is 25mm and corrosion is uniform.

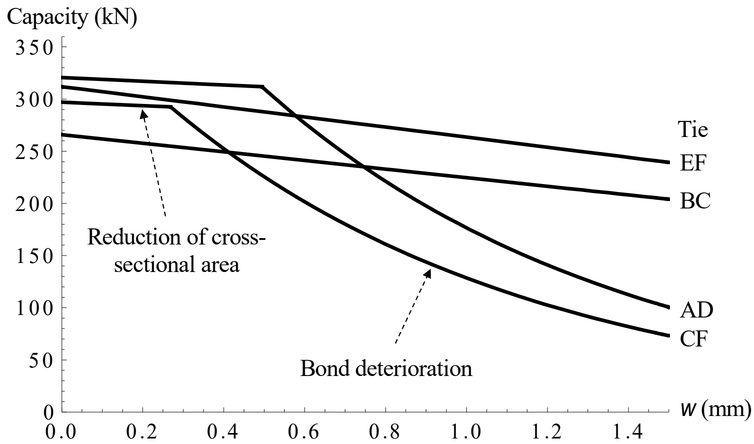


**Figure 9. Loss of capacity of the ties as function of crack width.**

If the thickness of the crack *w* is supposed to be constant for the entire D-Region, Figure 9 shows that the decay of the capacity is due to the reduction of the cross-sectional area of tie BC up to a $w \approx 0.4$mm. Beyond this value, the decay of the capacity is due to bond deterioration of tie CF. Figure 9 can also be used if different values of *w* are considered for each tie of the D-Region, what supposes a greater precision in the application of the method.

### 4.2. Capacity evolution of the nodes and struts

Table2shows the classification of each node and thickness of its most stressed side. According to the AASHTO LRFD-8 recommendations, nodal check is enough to verify both nodes andstruts. The thickness of the most stressed side times the breadth and the effective compression strength gives the capacity of both node and strut.

According to Eurocode 2[14], the maximum stress applicable to the edge of the nodes depends on the type of node:

$$\sigma_{Rd,\max} = k\upsilon f_{cd} = \begin{cases} \upsilon f_{cd} & for \quad CCC\ node \\ 0.85\upsilon f_{cd} & for \quad CCT\ node \\ 0.75\upsilon f_{cd} & for \quad CTT\ node \end{cases} \tag{21}$$

In Eq. (21) $\nu = 1 - f_{ck}/250$, being $f_{ck}$ the characteristic compressive strength of concrete and $f_{cd}=f_{ck}/\gamma_c$, being $\gamma_c$ the partial safety factor for concrete.

**Table2. Nodes characteristics**

| | A | B | C | D | E | F |
|---|---|---|---|---|---|---|
| Thickness of the most stressed side (mm) | 100 | 136.8 | 150 | 136.8 | 160 | 220.6 |
| Force acting in the most stressed side | 1.02 P | 1.43 P | 2.07P | 2.07P | 1.41P | 1.41P |
| Type of node | CCC | CCT | CTT | CCT | CCT | CTT |

The corrosion process produces a decay in the compressive strength of concrete due to softening and a reduction to the breadth of the struts because of the spalling of the cover. The first is expressed as function of the crack width while the second is considered to be a constant (Figure 6). Figure 10shows the capacity of the nodes as function of the crack width.

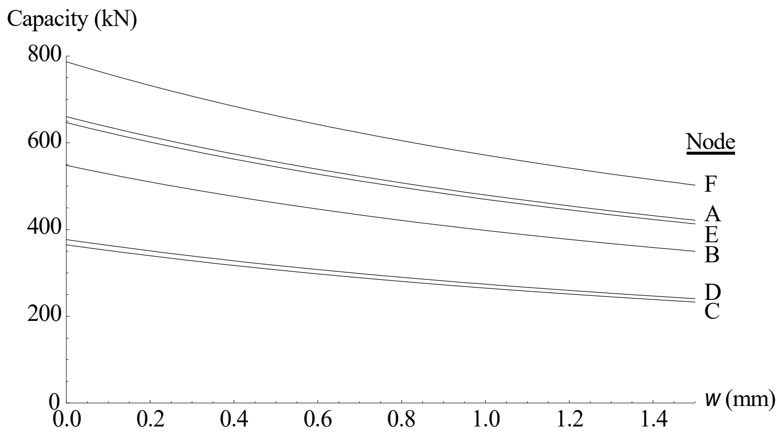


**Figure 10. Loss of capacity of the nodesas function of crack width.**

Comparison of Figure 9 and Figure 10 shows that in the studied case (D-Region in Figure 7) the capacity of the struts and nodes are always greater than those corresponding to the ties.

## 5. Experimental example of the proposed approach

In order to check the proposed model an experimental campaign from relevant literature has been analyzed. In Azam and Soudki [22,46] four RC deep beams with corroded longitudinal reinforcement were tested up to failure in three point bending. Deep beams are RC beams with a shear span to depth ratio ($a/d$) lower than 2.5. Design codes such as EC2 [14], AASHTO LRFD-8 [18]and ACI-318 [15]recommend S&T model for the design of RC deep beams because the arch action has a considerable contribution to its structural behavior. Two of the beams of the experimental campaign carried out in [22,46] have not transverse reinforcement (L specimens). The other two beams (LS specimens) have epoxy coated transverse reinforcement to prevent them from corrosion. Relevant information such as corrosion crack widths, dimensions of the support and loading plates and reinforcement detailing have been carefully examined.

The S&T model adopted is shown in Figure 11. In Figure 11, the dimension of the strut at the nodal zones of both the support and the loading plate are computed based on AASHTO LRFD-8 prescriptions. The capacity of each nodal zone is computed according to Eurocode 2 (see Eq. (21). Because the aim of the study is the assessment of the residual capacity of the D-Region, a partial safety factor for concrete equal to one is adopted (i.e. $\gamma_c$=1). The properties of the RC deep beams are the following [22,46]: shear span $a$ = 500 mm, effective depth $d$ = 307.5 mm, concrete cover $c$ = 30 mm, beam depth $h$ = 350 mm, beam breadth $b$ = 150 mm, width of support bearing plates$l_s$ = 62.5 mm, width of the loading plate $l_p$= 100 mm, available anchorage length $l_{b,av}$ = 584 mm, concrete strength $f_c$ = 47.3 MPa (authors have considered it to be the expected, or mean, value of the concrete compressive strength), longitudinal reinforcement 2-25M bars ($\phi$= 25.2 mm) and $f_y$= 400 MPa.

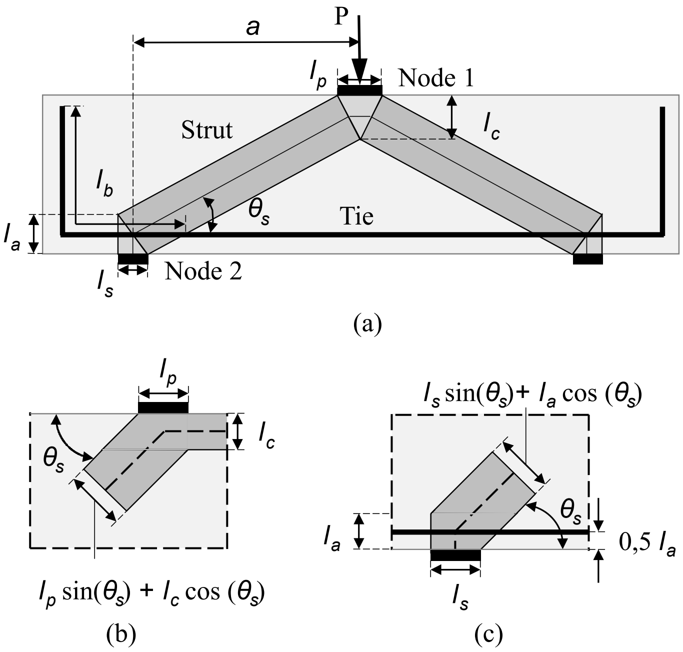


**Figure 11. Dimensions of S&T model employed to model the behavior of a RC deep beam. (a) S&T model, (b) strut anchored by bearing and reinforcement and (c) strut anchored by bearing and strut.**

The residual capacity of the corroded deep beams was estimated following the procedure shown in the previous section. The values of both experimental, $P_{exp}$, and predicted, $P_{corr}$, residual capacities of the four deep beams are in Table 3.

**Table 3. Comparison of predicted and experimental residual capacities of RC corroded deep beams presented in [22,46].**

| Specimen | $P_{corr}$(kN) | $P_{exp}$ (kN) | $P_{exp}/P_{corr}$ |
|---|---|---|---|
| L-5% | 413.24 | 476.40 | 1.15 |
| L-7.5% | 355.23 | 476.17 | 1.34 |
| LS-5% | 413.24 | 386.17 | 0.93 |
| LS-7.5% | 362.52 | 422.85 | 1.17 |

Figure 12 shows the loss of capacity of the tested specimens, notice that the only variation among the four beams is the level of corrosion, having the same geometry and reinforcement layout. The capacity of each component of the D-Region is shown as function of the crack width $w$. It can be seen that the decay of the capacity of the RC deep beam is due to the degradation of node 2 of the S&T model (see Figure 11 (a)).

The residual capacity of each corroded deep beam is computed following the proposed procedure. Let us consider for instance the specimen L-7.5%, shown by a circle in Figure 12. From the corrosion cracking map [46] two crack widths have been taken to evaluate this specimen: crack width at midspan $w_m$ = 1.5 mm and crack width at the supports nodal zone $w_s$ = 0.35 mm. These values are the equivalent crack widths corresponding to both reinforcing bars obtained as it is indicated in Figure 13.The capacity of the beam as function of the reduction of cross-sectional area of the tie (see circle with 3 in it in Figure 12) is calculated considering the crack width at midspan $w_m$. On the other hand, the capacity of the beam depending on both, bond deterioration of the tie (see circle with number two in it in Figure 12) and  capacity of node 2 (see circle with 1 in it, in Figure 12), have been estimated accounting for the crack width at the supports nodal zone $w_s$. Note that zone 1 is not affected by corrosion. Finally, the residual capacity of the corroded RC deep beam (specimen L-7.5% ) corresponds to the minimum of the values defined by circles 1, 2 and 3 of Figure 12 (in this case $P_{corr}$=355.23kN, corresponding to circle 1).The same procedure was applied for the rest of the specimens (see Figure 12).

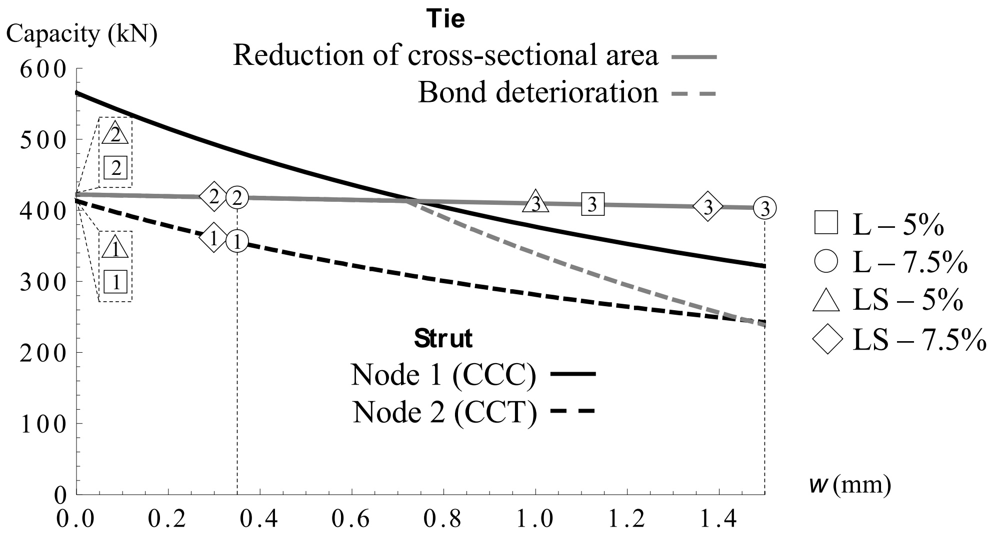


**Figure 12. Loss of capacity of the RC deep beams as function of crack width.**

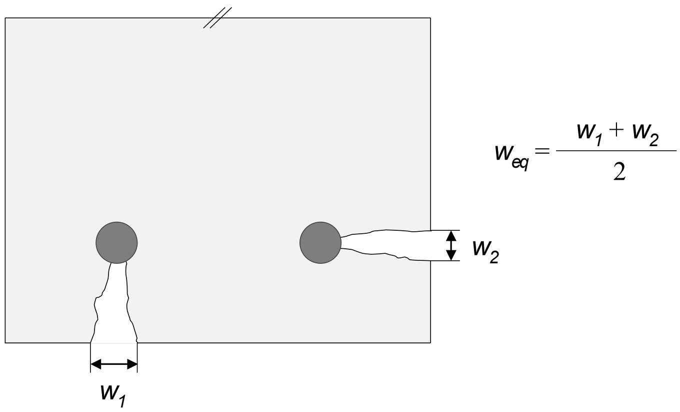


**Figure 13. Computation of the equivalent crack width in the tie composed by two reinforcing bars.**

According to Azam and Soudki[22,46]the experimental failure mode of the four corroded deep beams considered in the study was splitting of the strut.Because in the observations of the mentioned campaign [22,46]the bearing face of node 2 was neither observed nor considered, in this work nodes are only checked at the interface with the struts. No tension failure (bond or area reduction) of the corroded tie was observed in any of the tests in [22,46]. This is due to the good initial anchoring conditions of the longitudinal reinforcement. Table 3 shows that the predicted failure modes and values correlated very well with the experimental ones.

Relationships between crack width and corrosion level are used only in two degradation phenomena: the reduction of the bond strength and the reduction of cross-section area of the reinforcing bar. Due to this fact, differences may appear when considering the crack width or the level of corrosion.

## 6. Conclusions

A general procedure for the assessment of the residual structural capacity of D-Regions in RC structures affected by corrosion is proposed. The residual capacity is evaluated for monotonic loading. This method takes into account the reduction of the bond strength, the reduction of area of the reinforcing bar cross-section, the cracking of the concrete cover and the softening of concrete due to corrosion of the reinforcement. The necessary inputs for the implementation of the proposed procedure are expressed in terms of parameters that are obtained by Non-Destructive Tests and/or by visual inspection. The most important inputs of the method are the concrete corrosion-induced crack widths and their distribution, which can be easily obtained by a detailed visual inspection of the RC structure.

The anchorage length is a constant value in D-Regions and it cannot be increased. For this reason, the effect of the deterioration of bond strength between steel bars and the surrounding concrete has been taken into account by reducing the maximum tensile stress of the reinforcing bars. The worth of the method has been evaluated through its application to a real experimental campaign obtaining good similarities between the experimental and the predicted results. In addition, the computation of the residual capacity of a corroded RC half-joint has been developed with high detail. The proposed methodology can be considered as a good tool to assess the residual structural capacity of D-Regions of RC structures affected by corrosion.

## Acknowledgements

The present paper was financed by the Ministry of Science and Innovation – Spain under the research project RTI2018-101841-B-C21. The support is gratefully acknowledged.

## References

[1] R. Vedalakshmi, H. Dolli, N. Palaniswamy, Embeddable corrosion rate-measuring sensor for assessing the corrosion risk of steel in concrete structures, Struct. Control Heal. Monit. 16 (2008) 441–459.

[2] J. Rodriguez, L.M. Ortega, J. Casal, J.M. Diez, Corrosion of reinforcement and service life of concrete structures, Durab. Build. Mater. Components. 1 (1996) 117–126.

[3] R. Zhang, A. Castel, R. François, Concrete cover cracking with reinforcement corrosion of RC beam during chloride-induced corrosion process, Cem. Concr. Res. 40 (2010) 415–425. doi:10.1016/j.cemconres.2009.09.026.

[4] L. Chung, S.H. Cho, J.H.J. Kim, S.T. Yi, Correction factor suggestion for ACI development length provisions based on flexural testing of RC slabs with various levels of corroded reinforcing bars, Eng. Struct. 26 (2004) 1013–1026. doi:10.1016/j.engstruct.2004.01.008.

[5] H. Lin, Y. Zhao, J.Q. Yang, P. Feng, J. Ozbolt, H. Ye, Effects of the corrosion of main bar and stirrups on the bond behavior of reinforcing steel bar, Constr. Build. Mater. 225 (2019) 13–28. doi:10.1016/j.conbuildmat.2019.07.156.

[6] K. Stanish, R.D. Hooton, S.J. Pantazopoulou, Corrosion effects on bond strength in reinforced concrete, ACI Struct. J. 96 (1999) 915–921.

[7] D. Coronelli, P. Gambarova, Structural Assessment of Corroded Reinforced Concrete Beams: Modeling Guidelines, J. Struct. Eng. 130 (2004) 1214–1224. doi:10.1061/(ASCE)0733-9445(2004)130:8(1214).

[8] C. Maierhofer, H.W. Reinhardt, G. Dobmann, Non-Destructive evaluation of reinforced concrete structures: deterioration processes and standard test methods, CRC Press, 2010.

[9] A. Moustafa, E. Dehghan-Niri, A. Farhidzadeh, S. Salamone, Corrosion monitoring of post-tensioned concrete structures using fractal analysis of guided ultrasonic waves, Struct. Control Heal. Monit. 21 (2014) 438–448.

[10] W. Velez, F. Matta, P. Ziehl, Acoustic emission monitoring of early corrosion in

prestressed concrete piles, Struct. Control Heal. Monit. 22 (2015) 873–887.
[11] H. Debski, T. Sadowski, Modelling of microcracks initiation and evolution along interfaces of the WC / Co composite by the finite element method, Comput. Mater. Sci. 83 (2014) 403–411. doi:10.1016/j.commatsci.2013.11.045.
[12] J. Gajewski, T. Sadowski, Sensitivity analysis of crack propagation in pavement bituminous layered structures using a hybrid system integrating Artificial Neural Networks and Finite Element Method, Comput. Mater. Sci. 82 (2014) 114–117. doi:10.1016/j.commatsci.2013.09.025.
[13] J. Schlaich, K. Schäfer, M. Jennewein, Toward a consistent design of structural concrete, PCI J. 32 (1987) 74–150.
[14] CEN, Eurocode 2: Design of concrete structures - Part 1–1: General rules and rules for buildings UNE-EN 1992-1-1, European Committee for Standardization. Brussels, 2004.
[15] ACI Commitee 318, Building Code Requirements for Structural Concrete (ACI 318-19), Farmington Hills (MI): American Concrete Institute, 2019. doi:10.14359/51716937.
[16] H. Amini Najafian, R.L. Vollum, Design of planar reinforced concrete D regions with nonlinear finite element analysis, Eng. Struct. 51 (2013) 211–225. doi:10.1016/j.engstruct.2013.01.022.
[17] P. Marti, Basic tools of reinforced concrete beam design, ACI J. Proc. 82 (1985) 45–56.
[18] AASHTO, AASHTO LRFD Bridge Design Specifications 8th Edition, American Association of State Highway and Transportation Officials. Washington DC, 2017.
[19] H. Li, B. Li, R. Jin, S. Li, J.G. Yu, Effects of sustained loading and corrosion on

the performance of reinforced concrete beams, Constr. Build. Mater. 169 (2018) 179–187. doi:10.1016/j.conbuildmat.2018.02.199.

[20] J.F. Carbonell-Márquez, L.M. Gil-Martín, M.A. Fernández-Ruiz, E. Hernández-Montes, Procedure for the assessment of the residual capacity of corroded B-regions in RC structures, Constr. Build. Mater. 121 (2016) 519–534. doi:10.1016/j.conbuildmat.2016.06.029.

[21] L. Huang, H. Ye, X. Jin, N. Jin, Z. Xu, Corrosion-induced shear performance degradation of reinforced concrete beams, Constr. Build. Mater. 248 (2020) 118668. doi:10.1016/j.conbuildmat.2020.118668.

[22] R. Azam, K. Soudki, Structural performance of shear-critical RC deep beams with corroded longitudinal steel reinforcement, Cem. Concr. Compos. 34 (2012) 946–957. doi:10.1016/j.cemconcomp.2012.05.003.

[23] C. Suffern, A. El-Sayed, K. Soudki, Shear strength of disturbed regions with corroded stirrups in reinforced concrete beams, Can. J. Civ. Eng. 37 (2010) 1045–1056. doi:10.1139/L10-031.

[24] C. Cao, M.M.S. Cheung, Non-uniform rust expansion for chloride-induced pitting corrosion in RC structures, Constr. Build. Mater. 51 (2014) 75–81. doi:10.1016/j.conbuildmat.2013.10.042.

[25] H. Lin, Y. Zhao, J. Ožbolt, H.W. Reinhardt, Bond strength evaluation of corroded steel bars via the surface crack width induced by reinforcement corrosion, Eng. Struct. 152 (2017) 506–522. doi:10.1016/j.engstruct.2017.08.051.

[26] T. Vidal, A. Castel, R. François, Analyzing crack width to predict corrosion in reinforced concrete, Cem. Concr. Res. 34 (2004) 165–174. doi:10.1016/S0008-8846(03)00246-1.

[27] J.A. González, C. Andrade, C. Alonso, S. Feliu, Comparison of rates of general

corrosion and maximum pitting penetration on concrete embedded steel reinforcement, Cem. Concr. Res. 25 (1995) 257–264. doi:10.1016/0008-8846(95)00006-2.

[28] C. Alonso, C. Andrade, J. Rodriguez, J.M. Diez, Factors controlling cracking of concrete affected by reinforcement corrosion, Mater. Struct. 31 (1998) 435–441.

[29] A. Castel, I. Khan, R. François, R.I. Gilbert, Modeling steel concrete bond strength reduction due to corrosion., ACI Struct. J. 113 (20169) 937–982. doi:10.14359/51688925.

[30] M. Prieto, P. Tanner, C. Andrade, Multiple linear regression model for the assessment of bond strength in corroded and non-corroded steel bars in structural concrete, Mater. Struct. Constr. 49 (2016) 4749–4763. doi:10.1617/s11527-016-0822-8.

[31] K. Bhargava, A.K. Ghosh, Y. Mori, S. Ramanujam, Corrosion-induced bond strength degradation in reinforced concrete. Analytical and empirical models, ACI Mater. J. 104 (2007) 594–603. doi:10.1016/j.nucengdes.2007.01.010.

[32] K. Bhargava, A.K. Ghosh, Y. Mori, S. Ramanujam, Suggested empirical models for corrosion-induced bond degradation in reinforced concrete, J. Struct. Eng. 134 (2008) 221–230.

[33] G.J. Al-Sulaimani, M. Kaleemullah, I.. Basunbul, Rasheeduzzafar, Influence of corrosion and cracking on bond behaviour and strength of reinforced concrete members, ACI Struct. J. 87 (1990) 220–231.

[34] FIB, Model Code 2010. Model Code 2010 – Final draft, vol. 1. Fib Bulletin No. 65. Lausanne: International Federation for Structural Concrete, 2012.

[35] F.J. Vecchio, M.P. Collins, The modified compression-field theory for reinforced concrete elements subjected to shear, ACI J. Proc. 83 (1986) 219–231.

[36] T.N. Tjhin, D.A. Kuchma, Computer-Based Tools for Design by Strut-and-Tie Method : Advances and Challenges, ACI Struct. J. 99 (2002) 586–594.

[37] M. Capè, Residual service-life assessment of existing R/C structures, MS thesis, Chalmers University of Technology, Göteborg (Sweden) and Milan University of Technology (Italy), 1999.

[38] C. Cao, M.M.S. Cheung, B.Y.B. Chan, Modelling of interaction between corrosion-induced concrete cover crack and steel corrosion rate, Corros. Sci. 69 (2013) 97–109. doi:10.1016/j.corsci.2012.11.028.

[39] Y.G. Du, A.H.C. Chan, L.A. Clark, X.T. Wang, F. Gurkalo, S. Bartos, Finite element analysis of cracking and delamination of concrete beam due to steel corrosion, Eng. Struct. 56 (2013) 8–21. doi:10.1016/j.engstruct.2013.04.005.

[40] Y.C. Ou, N.D. Nguyen, Influences of location of reinforcement corrosion on seismic performance of corroded reinforced concrete beams, Eng. Struct. 126 (2016) 210–223. doi:10.1016/j.engstruct.2016.07.048.

[41] C. Higgins, W.C. Farrow, T. Potisuk, T.H. Miller, S.C. Yim, G.R. Holcomb, S.D. Cramer, B.S. Covino, S.J. Bullard, S.A. Matthes, Shear capacity assessment of corrosion-damaged reinforced concrete beams, Technical Report. Oregon Department of Transportation, 2003.

[42] G.N.J. Kani, The riddle of shear failure and its solution, ACI J. Proceedings1. 61 (1964) 441–468.

[43] M.A. Fernández-Ruiz, L.M. Gil-Martín, E. Hernández-Montes, Structural Performance of RC Beams containing Tension-Only Nodes, Int. J. Concr. Struct. Mater. 12 (2018). doi:10.1186/s40069-018-0228-9.

[44] E. Hernández-Montes, L.M. Gil-Martín, Hormigón Armado y Pretensado, Concreto reforzado y preesforzado, 2ª edición, Garceta. Madrid, 2014.

[45] B. Martin, D. Sanders, Verification and implementation of strut-and-tie model in LRFD bridge design specifications, 2007.

[46] R. Azam, Behaviour of shear critical RC beams with corroded longitudinal steel reinforcement, MS thesis, University of Waterloo (Canada), 2010.